Arabian Journal of Chemistry (2021) **14**, 103084

King Saud University

Arabian Journal of Chemistry

www.ksu.edu.sa
www.sciencedirect.com

ORIGINAL ARTICLE

Evaluation of the genotoxicity and mutagenicity of isoeleutherin and eleutherin isolated from *Eleutherine plicata* herb. using bioassays and *in silico* approaches

Ana Laura Gadelha Castro [a], Jorddy Neves Cruz [b], Daniele Ferreira Sodré [c], Juliana Correa-Barbosa [a], Rufine Azonsivo [a], Mozaniel Santana de Oliveira [b], José Edson de Sousa Siqueira [d], Natasha Costa da Rocha Galucio [e], Marcelo de Oliveira Bahia [f], Rommel Mario Rodriguez Burbano [e,f], Andrey Moacir do Rosário Marinho [d], Sandro Percário [g], Maria Fâni Dolabela [a,h], Valdicley Vieira Vale [h,*]

[a] *Programa de Pós-Graduação em Ciências Farmacêuticas, Universidade Federal do Pará, Belém, PA, Brazil*
[b] *Programa de Pós-graduação em Biodiversidade e Biotecnologia (BIONORTE), Universidade Federal do Pará, Brazil*
[c] *Faculdade de Farmácia, Universidade Federal do Pará, Belém, PA, Brazil*
[d] *Programa de Pós-Graduação em Química, Universidade Federal do Pará, Belém, PA, Brazil*
[e] *Programa de Pós-Graduação em Genética e Biologia Celular, Universidade Federal do Pará, Belém, PA, Brazil*
[f] *Programa de Pós-Graduação em Neurociências e Biologia Celular, Universidade Federal do Pará, Belém, PA, Brazil*
[g] *Bionorte, Universidade Federal do Pará, Belém, PA, Brazil*
[h] *Programa de Pós-graduação em Inovação Farmacêutica, Universidade Federal do Pará, Belém, PA, Brazil*

Received 24 November 2020; accepted 10 February 2021
Available online 23 February 2021

KEYWORDS

Genotoxicity;
Mutagenicity;
Naphthoquinones

Abstract The biological activities of *Eleutherine plicata* Herb. have been linked to isoeleutherin and eleutherin naphthoquinones. However, there are few reports in the literature regarding the cytotoxic and genotoxic potential of these compounds. There are reports in the literature that the inhibition of topoisomerase II (TOPO II) is involved in the toxicity of these compounds, as it causes damage to cellular DNA. In this study, we evaluated the genotoxicity and mutagenicity of these compounds using a bioassay on *Allium cepa* and micronuclei. We also performed an *in sil-*

* Corresponding author.
E-mail addresses: rommel@ufpa.br (R.M.R. Burbano), andrey@ufpa.br (A.M. do Rosário Marinho), percario@ufpa.br (S. Percário), percario@ufpa.br (M.F. Percário).
Peer review under responsibility of King Saud University.

Production and hosting by Elsevier

https://doi.org/10.1016/j.arabjc.2021.103084

ico evaluation of the toxic potential of these molecules using the PreADMET server. Finally, to assess whether binding to TOPO II influences toxicity, we used molecular docking and molecular dynamics (MD) simulations. *In silico* studies of prediction have demonstrated the identical toxicity profiles and mutagenicity for Algae, Daphnia, and fish. However, eleutherin proved to be more genotoxic, increasing the mitosis index, aberration index, and micronucleus, bud, and bridge were observed during metaphase. The results of docking and MD simulations demonstrated that the compounds were able to interact with the residues present in the enzyme binding pocket. Throughout the MD trajectories, the compounds showed molecular stability and the free energy results prove that the compounds formed a stable complex with TOPO II. These results provide new insights into the genotoxic and mutagenic potential of isoeleutherin and eleutherin.

1. Introduction

E. plicata is a native American plant also found in different tropical countries (Prameela et al., 2018). Phytochemical studies conducted with *E. plicata* suggest that isoeleutherin (Fig. 1A) and eleutherin (Fig. 1B) are the major naphthoquinones produced by the species, and may serve as chemical markers (Malheiros et al., 2015; Paramapojn et al., 2008).

This plant has been popularly used to treat malaria, diseases in the gastrointestinal tract, and diseases caused by bacteria, fungi and other parasites (Couto et al., 2016). The biological activities of this plant have been related to naphthoquinones such as isoeleutherin and eleutherin. (Hara et al., 1997; Le et al., 2013; Vale et al., 2020).

The mechanism of action of naphthoquinones involves the formation of reactive oxygen species (ROS) such as hydrogen peroxide (H_2O_2), superoxide radical anion ($O_2^{\cdot-}$), and hydroxyl radical ($HO^{\cdot}$) induced by the bioreduction of the quinonic complex, resulting in the oxidative stress of cells or induction of apoptosis by inhibiting the topoisomerase complex. As a consequence, cells lose their ability to repair, determining the potential of these compounds to cause DNA damage by breaking single and/or double strands. There are studies that signal intercalation in the double helix of DNA and alkylation of the nucleotides (Campos et al., 2012; Da Silva et al., 2003). However, studies on human hepatoma (HepG2) cells have shown that isoeleutherin has a low genotoxic potential (Sunassee et al., 2013).

Eleutherin has TOPO II inhibitory activity. Substances that inhibit topoisomerase, in general, bind to two receptors (Wang, 1996), stabilizing the enzyme-DNA complex after the cutting stage and before the DNA is recomposed, preventing the continuation of normal functions and leading to death cellular (Bamford et al., 2000; Da Silva et al., 2003).

As stated earlier, some mechanisms may be involved in the toxicity of naphthoquinones, such as oxidative stress and inhibition of TOPO II. Reactive oxygen species can cause severe DNA damage to cells and may lead to chromosomal changes (Bamford et al., 2000). Studies with Alium cepa and micronucleo can show this damage. In addition, *in silico* studies can assess the role of TOPO II in the toxicity of these compounds.

In this study, we used the *Allium cepa* bioassay and micronuclei to assess the genotoxic and mutagenic potential of isoeleutherin and eleutherin. To assess the toxicity of these compounds, we used an *in silico* approach with the PreADMET server. Finally, we evaluated the likely mechanism of interaction of molecules with TOPO II by means of molecular docking and molecular dynamics simulations.

2. Material and methods

2.1. General experimental procedures

Nuclear magnetic resonance (NMR) spectra were measured using a Bruker Brucker Advance DPX 400 MHz NMR spectrometer (Karlsruhe, Germany). Chromatographic column was prepared using silica gel 60 (0.063–0.200 mm, 70–230 mesh, Merck, Germany). Hexane, dichloromethane, ethyl acetate, and methanol (Isofar, Brazil) were used as the mobile phase. Ethanol 96°G (Santa Cruz®) for the preparation of the ethanolic extract. Allium cepa (Baia Periforme, ISLA®), Petri dish (Global plast 90 × 15 mm), filter paper (Unifil 90 mm), colchicine powder (Merck C9754-100 mg), slides (Global Glass), optical microscope (Nikon E200), deionized water (Milli-Q® IQ 7003), Carnoy fixative (Dinamica®), Schiff reactive PA orcein dye (Exodo®) were used in the Allium cepa assay. RPMI-1640 (Gibco, Thermo Fisher Scientific, USA) and fetal bovine serum (Laborclin, BRA), streptomycin (Sigma, USA), penicillin (Sigma, USA), CO_2 incubator (Laboven, BRA) were used for cell culture HepG2 and Doxorubicin (Sigma, USA), cytochalasin-B (Sigma, USA), KCl (Merck S/A, DE), Methanol (Merck S/A, DE), acetic acid (Merck S/A, DE), formaldehyde (Merck S/A, DE), Giemsa 5% (Merck S/A, DE), slides (Global Glass), optical microscope (Nikon E200) for the Micronucleus Test with cytokinesis block.

2.2. Experimental procedures

2.2.1. Plant material and extraction procedure

E. plicata bulbs were collected in the municipality of Tracuateua - PA, BR 308, Lat. −1.1436, Long. −46.9511 west, in June 2015. The botanical identification was carried out by Dra. Márlia Regina Coelho Ferreira, and the exsiccata was deposited at the Herbário João Murça Pires (MG) of the Paraense Museum "Emílio Goeldi" under the MG record. 202631.

The bulbs were washed, dried in a forced air oven, ground, and extracted with 96° ° GL ethanol, followed by concentration in a rotary evaporator, and the ethanolic extract (EEEP) was obtained. This was subjected to re-extraction under reflux (Vale et al., 2015) and the dichloromethane fraction was fractionated in a column, with isoeleutherin and eleutherin isolated, identified by nuclear magnetic resonance, obtaining the

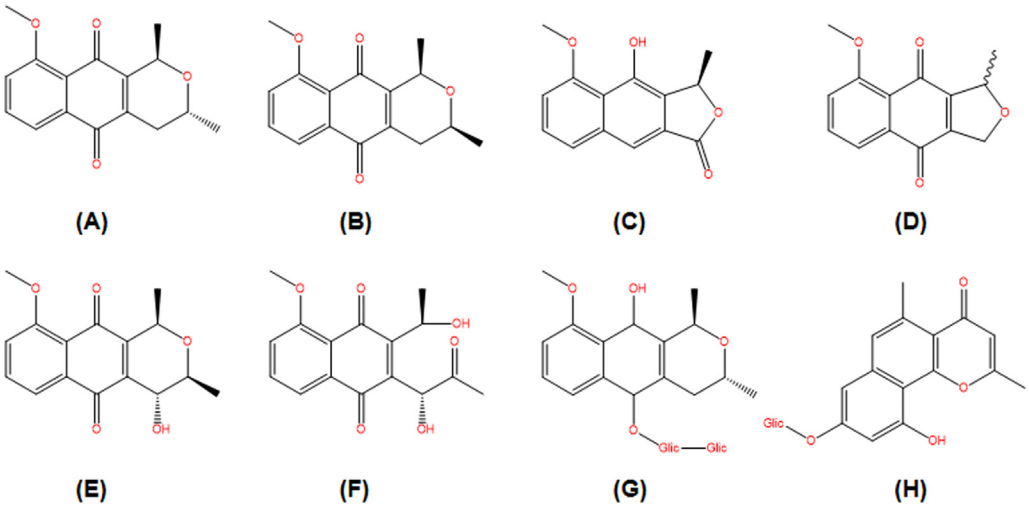

Fig. 1 Chemical constituents isolated from *Eleutherine plicata*.: (A) isoeleutherin; (B) eleutherin; (C) eleutherol; (D) eleutherinone; (E) (R) −4-Hydroxyeleutherine; (F) eleuthrone; (G) isoeleuthoside C; (H) eleutherinol-8-O-β-D-glucoside.

spectra described below. The extract, dichloromethane fraction, and the isolated products were monitored using TLC (silica gel) eluted with n-hexane: ethyl acetate (8: 2) and developed with sulfuric anisaldehyde.

Isoeleutherin - ^{1}H NMR 400 MHz ($CDCl_3$): δ 1.32 (3H, d, J = 8.0 Hz, Me-3), δ 1.52 (3H, d, J = 8.0 Hz, Me-1), δ 2.22 (1H, dq, J = 4.0; 16.0 Hz, H4-ax), δ 2.68 (1H, dd, J = 4.0; 16.0 Hz, H-4 eq), δ 3.99 (3H, s, OMe-9), δ 4.99 (1H, m, H-1), δ 7.27 (1H, d, J = 8.0 Hz, H-6), δ 7.63 (1H, t, J = 8.0; 16 Hz, H-7), δ 7.72 (1H, d, J = 8.0 Hz, H-8). ^{13}C NMR 100 MHz ($CDCl_3$): δ 19.93 (Me-3), δ 21.67 (Me-1), δ 29.98C-4), δ 56.62 (OMe-10), δ 62.64 (C-3), δ 67.58 (C-1), δ 117.99 (C-8), δ 119.28 (C-7), δ 119.93 (C-4a), δ 134.26 (C-11a), δ 134.87 (C-11a), δ 139.54 (C-5a), δ 148.23 (C-9a), δ 159.90 (C-9), δ 182.90 (C-5), δ 184.42 (C-10) (Fig. S1)

Eleutherin - ^{1}H NMR 400 MHz ($CDCl_3$): δ 1.36 (3H, d, J = 8.0 Hz, Me-3), δ 1.53 (3H, d, J = 8.0 Hz, Me-1), δ 2.19 (1H, dq, J = 4.0; 16.0 Hz, H4-ax), δ 2.74 (1H, dt, J = 4.0; 16.0 Hz, H-4 eq), δ 3.58 (1H, m, H-3), δ 3.99 (3H, s, OMe-9), δ 4.85 (1H, m, H-1), δ 7.27 (1H, d, J = 8.0 Hz, H-6), δ 7.63 (1H, t, J = 8.0; 16 Hz, H-7), δ 7.72 (1H, d, J = 8.0 Hz, H-8). ^{13}C NMR 100 MHz ($CDCl_3$): δ 20.92 (Me-3), δ 21.38 (Me-1), δ 30.05 (C-4), δ 56.59 (C-9), δ 68.70 (C-3), δ 70.40 (C-1), δ 117.93 (C-8), δ 119.12 (C-7), δ 134.66 (C-6), δ 120.46 (C-4a), 134.15 (C-11a), δ 140.08 (C-5a), δ 148.83 (C-9a), δ 159.54 (C-9), δ 183.84 (C-5), δ 184.15 (C-11) (Fig. S2).

2.2.2. Test Allium cepa

The seeds of the species *Allium cepa* were used for the evaluation of the genotoxic and mutagenic effects of the samples. The seeds were placed in petri dishes lined with filter paper and then germinated in deionized water until the roots reached 1–1.5 cm in length. After this procedure, the roots were transferred to other petri dishes, each one containing different concentrations of the test samples, the colchicine solution (positive control), and Milli-Q water (negative control), for 24 h. After this time period (24, 48, and 72 h), the roots were fixed in Carnoy solution (3 parts of absolute ethanol to 1 part of glacial acetic acid – v:v), for 6 to 18 h at room temperature, and later stored in a refrigerator, in freshly prepared Carnoy solution, until use (Bianchi et al., 2015).

The previously fixed roots were washed in three baths of distilled water for 5 min each and treated with Schiff's reactive P.A orcein dye. With the meristems stained and washed in running water, the slides were prepared using the common crushing method, for chromosomal aberrations (genotoxicity test), micronuclei (mutagenicity test), cell death, and mitotic index (cytotoxicity test). A total of 1000 cells per slide were analyzed, totaling 5000 cells per treatment. The observation was made under light microscopy at 400× magnification (Bianchi et al., 2015). Genetic analysis of the test samples in the *A. cepa* cells was also performed, where the presence of micronuclei was observed (Bagatini et al., 2007).

2.2.3. Cell culture and Cytokinesis-Block Micronucleus Test (CBMN)

HepG2 cells were cultured in RPMI-1640 medium supplemented with 10% fetal bovine serum – FBS, 100 μg/mL streptomycin and 60 μg/mL penicillin. This strain was grown in culture bottles, stored in a CO_2 gas incubator, at 37 °C in a humid atmosphere with 5% CO_2.

For the Micronucleus Test with cytokinesis block, 2×10^5 cells/mL were seeded in a 12-well plate, and after 20 h in culture, the cells were treated with isoeleutherin (15.55 μg/mL, 7.77 μg/mL and 3.88 μg/mL). Negative control (cells and culture medium) and positive control (0.02 μg/mL doxorubicin) were used. After 24 h, 3 μg/mL of cytochalasin-B (CitB) was added. After 24 h with CitB (72 h of incubation after the beginning of the culture), the cells were trypsinized and centrifuged at 1000 rpm for 5 min. Then, 5 mL of cold hypotonic solution (KCl 0.075 M) was added, and homogenization and centrifugation at 1000 rpm for 5 min was performed. The supernatant was discarded and 5 mL of 5:1 fixative (5 parts of methanol: 1 part of acetic acid) freshly prepared and 3 drops of formaldehyde were added. The contents were centrifuged at 1000 rpm for 5 min, the supernatant was discarded, and the slides were prepared. The slides were stained with Giemsa 5% for 5 min (Fenech and Morley, 1985). Finally, the analysis of several parameters such as the conventional micronucleus and the

Nuclear Division Index (NDI) was performed using a light microscope under 1000× magnification.

For the analysis of the micronucleus and calculation of the Nuclear Division Index (IDN), the criteria of Fenech, 2000 were used (Fenech, 2000). The statistical analysis was performed using ANOVA followed by the Tukey test for multiple comparisons. P values less than or equal to 0.05 were considered statistically significant.

2.3. In silico methodology

2.3.1. In silico prediction of toxicity

For toxicological predictions using the PreADMET software, a software package for prediction of various properties based on designed structure of chemical compounds (Lee et al., 2002), the toxicity in algae, microcrustacean Daphnia sp., medaka and minnow fish, the mutagenicity (Ames test), carcinogenicity, and changes in rats and mice were considered. The following parameters were used as criteria for assessing toxicity: Toxicity to Algae: Toxic: <1 mg/L; Non-toxic: >1 mg/L (Costa et al., 2008); Toxicity to Daphnia sp: Toxic: <0.22 μg/mL; Non-toxic: >0.22 μg/mL (Guilhermino et al., 2000); Toxicity to Medaka and Minnow fish: Very toxic: <1 mg/L; Toxic: 1–10 mg/L; Harmful: 10–100 mg/L; Non-toxic: >100 mg/L (Zucker, 1985).

2.3.2. Molecular docking

The initial complexes of type TOPO II interacting with eleutherin and isoeleutherin were obtained through molecular docking using the Molegro Virtual Docker (MVD) 5.5 software (Thomsen and Christensen, 2006). For docking, the MolDock score function at a grid resolution of 0.30 and the MolDock SE algorithm were used. MolDock Score is a scoring function to rank the poses of ligands that have the greatest affinity with the active site of proteins. The structure of TOPO II was obtained from the Protein Data Bank (PDB) (PDB ID: 1ZXM) (Wei et al., 2005). The molecular structure of the compounds was designed with GaussView 5 (Dennington et al., 2009), the structures were optimized with Gaussian 16 using density functional theory, with the B3LYP/6-31G * basis sets (Becke, 1993; Lee et al., 1988).

2.3.3. Molecular Dynamics (MD) simulation

The starting structures for the MD simulations were obtained from the results of molecular docking. The MD simulations were run with an explicit solvent using the Amber 16 package (Araújo et al., 2020; Neto et al., 2020; Salomon-Ferrer et al., 2013). TOPO II protein was treated with the 14SB force field (Maier et al., 2015). The protonation status of its residues was evaluated at neutral pH using the PROPKA server (Dolinsky et al., 2004; Li et al., 2005). The atomic charge of the eleutherin and isoeleutherin ligands was calculated using the Restrained Electrostatic Potential (RESP) protocol, with the HF/6-31G* basis sets (Cornell et al., 1993). The parameters of the ligands were created using the Antechamber module (Wang et al., 2006) and General Amber Force Field (GAFF) (Wang et al., 2004). Protein-ligand systems were built using tLEaP. These systems were immersed in a truncated octahedron periodic box containing water molecules described by the TIP3P model (Jorgensen et al., 1983). Counter-ions were added to neutralize the partial load of the systems.

We used the sander. MPI for the four stages of energy minimization. In each of these stages, it took 2000 cycles using the steepest descent method and 4000 cycles using the conjugate gradient algorithm. In the first stage the hydrogen atoms of the water molecules were optimized; then, the ions and the water molecules were minimized; in the third stage, the hydrogen atoms of the protein and in the last step the solute and the solvent underwent the process of energy minimization. Three heating steps were used for a total time of 800 picoseconds to raise the system temperature to 300 K using NVT ensemble. To equilibrated the systems, we performed 2 ns simulations with NPT ensemble. Finally, for each system, we performed 100 ns of MD of production.

Particle Mesh Ewald (Darden et al., 1993) method was used for the calculation of electrostatic interactions. Bonds involving hydrogen atoms were restricted with the SHAKE (Ryckaert et al., 1977) algorithm. Temperature control was performed with the Langevin thermostat (Lzaguirre et al., 2001) within collision frequency of 2 ps^{-1}.

2.3.4. Binding affinities calculations

To estimate the A_{2A} receptor-ligand affinity energy was calculated with Molecular Mechanics/Generalized Born Surface Area (MM/GBSA) method (Kollman et al., 2000; Neves Cruz et al., 2020). For our calculations we used 500 snapshots of the last 5 ns of MD simulation.

The free energy was estimated according to Eq. (1):

$$\Delta G_{bind} = \Delta E_{MM} + \Delta G_{solv} - T\Delta S \quad (1)$$

ΔG_{bind} is the affinity energy resulting from the sum of the total energy in the gas phase (ΔE_{MM}), free energy of solvation (ΔG_{solv}) and entropy ($T\Delta S$).

ΔE_{MM} is the sum of $\Delta E_{internal}$ (connections, angles and dihedra), $\Delta E_{electrostatic}$ (electrostatic contributions) and ΔE_{vdW} (van der Waals contributions), according to Eq. (2):

$$\Delta E_{MM} = \Delta E_{internal} + \Delta E_{electrostatic} + \Delta E_{vdw} \quad (2)$$

ΔG_{solv} can be obtained from the resolution of Eq. (3):

$$\Delta G_{solv} = \Delta G_{GB} + \Delta G_{SASA} \quad (3)$$

where the polar contributions (ΔG_{GB}) is calculated using either the GB model and the non-polar contributions (ΔG_{SASA}) are determined from the calculation of the solvent accessible surface area (SASA).

3. Results and discussions

3.1. Phytochemical studies and isolation

The ethanol extract was fractionated by reflux, obtaining three fractions (data not shown), of which the dichloromethane fraction was used for fractionation. Fig. 2 shows the bands obtained, together with their retention factor values (Rf), showing the isolation of the isoeleutherin products (Rf = 0.40, Fig. 2E) and eleutherin (Rf = 0.50, Fig. 2D). These molecules were identified using nuclear magnetic resonance, and the peak displacement values were compared with data from the literature confirming the isolation of the isomers of these naphthoquinones that had previously been identified in the plant species (Hara et al., 1997; Malheiros et al., 2015).

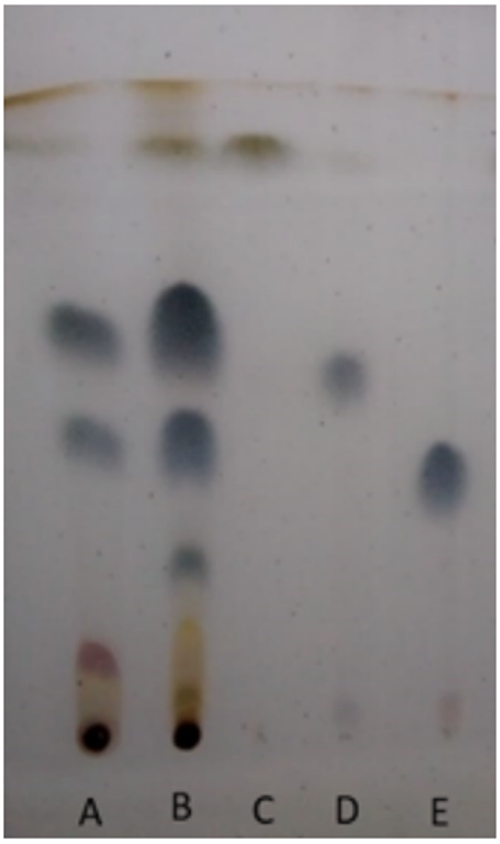

Fig. 2 Chromatographic profile obtained from *E. plicata*. Chromatographic conditions: stationary phase-silica gel (TLC); Mobile phase: n-hexane: ethyl acetate (8:2); revealed with sulfuric anisaldehyde. A – ethanol extract of *E. plicata*; B – *E. plicata* dichloromethane fraction; C – fraction 15; D – eleutherin; E – isoeleutherin.

3.2. Toxicity studies

The *in silico* toxicity study performed with the PreADMET software suggests that isoeleuterin and eleutherin are toxic to algae and Daphnia, and extremely toxic to medaka and minnow. Regarding cytotoxicity to hERG, the two compounds presented a medium risk and appeared to be carcinogenic only for rats (Table 1).

Studies on the toxicity of naphthoquinones in marine organisms are still scarce. However, a study demonstrated that, in concentrations of 0.8 to 31.2 mg/L, 1,4-naphthoquinone (2- (2,4-dimethoxyphenyl) naphthalene-1,4-dione (8), 2-(2 , 4,6-trimethoxyphenyl) naphthalene-1,4-dione (9), and N- [4-(1,4-dioxo-1,4-dihydronaphthalen-2-yl) −3-met hoxyphenyl]acetamide) was not toxic to zebrafish (Janeczko et al., 2018), however the 1,4-naphthoquinones in this study were very toxic to medaka and minnow fish, and toxic to other marine organisms, differences that can be explained by the differences between the compounds, but further studies are needed to verify these differences.

Campos et al. (2016) evaluated the cytotoxicity of these molecules in different tumor and normal cell lines, observing that the cytotoxic effect varies according to the line used, and eleutherin was more cytotoxic for the glioma lines (U251, IC50 = 2.8 μg/μg/mL) and breast cancer cell lines (MCF-7, IC50 = 4.8. μg/mL) compared to isoeleutherin; however, a similar profile was observed in the leukemia strain (Campos et al., 2016). Isomers are known to show significant differences in the toxicity and biological activities.

In the comet assay, it was observed that the damage index (ID) by isoeleutherin was high (ID = 2.07), but was slightly lower than that by doxorubicin (ID = 2.22). This suggests that the damage caused by isoeleutherin can be repaired.

The *Allium cepa* test was performed in order to understand the genotoxic effects of isoeleutherin and if stereoisomeric changes interfere with genotoxicity. In this test, changes in the mitotic index (MI), abnormalities in the mitotic cycle, multinucleated cells, linked nuclei, and the aberration index (TA) were evaluated.

Isoeleutherin, at all concentrations evaluated, did not significantly interfere with the mitotic index and did not cause anomalies in the mitosis cycle, and no micronucleated cells were observed. However, there were aberrations, and the exposure time interfered with the aberration index (Table 2). The aberrations occurred mainly in anaphase, with bridges, multinucleated cells, and mitotic irregularities. This fact may be related to the occurrence of interactions and/or inhibitions of essential structures that play a role in the formation of the mitotic spindle, preventing the succession of the cell division process, culminating in chromosomal abnormalities.

There was a pronounced increase in MI over 72 h in eleutherin. The indices of aberrations caused by eleutherin at concentrations of 12.5 and 25.0 μg/mL were higher than the indices of isoeleutherin (Table 2). Unlike isoeleutherin, cells treated with eleutherin (25 μg/mL) showed micronucleus, bud, and mitotic irregularities during metaphase (Fig. 3). In contrast, in anaphase, changes similar to those caused by isoeleutherin were observed. These results reinforce the hypothesis that eleutherin has a greater toxic potential than isoeleutherin.

Table 1 *In silico* toxicity of isoeleutherin and eleutherin.

Molecule	CL59 (mg/L)		DL50 (mg/L)		Cytotoxicity	Mutagenicity		Carcinogenicity	
	Algae	Daphinia	Medaka	Minnow	hERG	+TA100 NA	TA 100 RLI	Rats	Mouse
Isoeleutherin	T	T	MT	MT	MR	+	–	+	–
Eleutherin	T	T	MT	MT	MR	+	–	+	–

T – Toxic; NT – non-toxic; MT – very toxic; MR – medium risk; BR – low risk; + positive; – negative; TA 100 NA – *Salmonella typhimurium* hisG46 mutation without the addition of fraction S9; TA 100 RLI – *Salmonella typhimurium* clone hisG46 mutation with the addition of S9 fraction

Table 2 Determination of mitotic index and aberrations of cells treated with eleutherin and isoeleutherin.

Samples	Mitotic index (MI %)			Aberration index (TA %)		
	24 h	48 h	72 h	24 h	48 h	72 h
H_2O	3.99	NA	2.16	0.02	NA	0.15
Colchicine						
1.6 μg/mL	1.59	2.66	2.93	0.05	0.24	0.34
3.12 μg/mL	6.79	6.20	6.98	0.35	0.66	0.34
6.25 μg/mL	5.91	5.66	2.84	1.32	0.78	0.41
12.5 μg/mL	NA	5.28	5.83	ND	0.85	0.95
25 μg/mL	5.74	3.48	ND	0.95	0.92	NA
Eleutherin						
1.6 μg/mL	3.71	3.66	3.43	0.09	0.09	0.07
3.12 μg/mL	4.13	3.16	3.61	0.05	0.11	0.09
6.25 μg/mL	3.93	3.27	4.06	0.21	0.13	0.19
12.5 μg/mL	4.90	3.89	6.54	0.21	0.11	1.21
25 μg/mL	4.64	4.22	10.05	0.76	0.65	1.43
Isoeleutherin						
1.6 μg/mL	ND	2.73	3.02	ND	0.08	0.07
3.12 μg/mL	3.00	3.38	3.30	0.03	0.09	0.05
6.25 μg/mL	2.94	3.55	ND	0.07	0.05	NA
12.5 μg/mL	3.75	3.67	3.33	0.21	0.09	0.15
25 μg/mL	4.05	3.58	3.54	0.09	0.17	0.15

NA: Not evaluated.

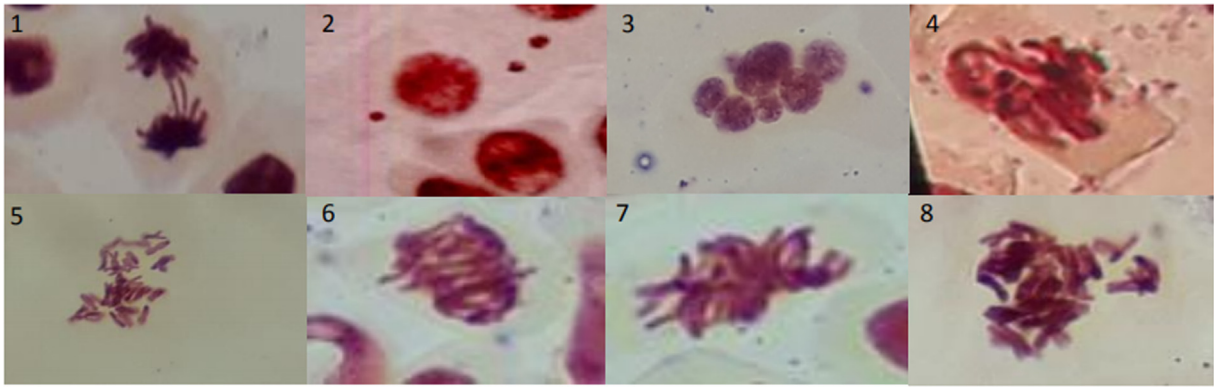

Fig. 3 Phenomena found in the *Allium cepa* test after treatment with eleutherin. 1: bridge; 2: micronucleus; 3: multinucleated cell; 4–8: mitotic irregularities.

Due to the fact that isoeletherin is less genotoxic than eleutherin, we decided to do the micronucleus test with this sample, as it is more promising. Table 3 shows the result, in which the percentage of micronuclei in the HepG2 strain was concentration-dependent and the same occurs with the nuclear division index. Previous studies showed that quinones, fractions and extracts containing this metabolite have the potential to induce cytogenetic damage (Babula et al., 2006; Kiran Aithal et al., 2009; Kumar et al., 2009; SivaKumar et al., 2005). In general, this damage index/micronucleus percentage has a direct relationship with the sample concentration, and the formation of micronuclei by Isoeleutherin was less than that of the positive control ($p < 0.05$).

Because it is a naphthoquinone, isoeleutherin has the ability to induce the formation of reactive oxygen species (ROS) and the depletion of glutathione (GSH) in MCF-7 cells, and subse-

Table 3 Determination of micronuclei and nuclear division index of isoeleutherin and their respective standard deviations (SD).

Sample	Concentration (μg/mL)	Frequency of micronuclei (%)	Nuclear Division Index
Isoeleutherin	15.55	4.03 ± 0.25	1.36 ± 0.16
	7.77	2.90 ± 0.20	1.39 ± 0.15
	3.88	2.10 ± 0.36	1.51 ± 0.14
Negative control	–	2.40 ± 0.56	1.94 ± 0.01
Doxirrubicin	0.02	36.07 ± 1.36	1.87 ± 0.05

quent cell death (Lin et al., 2007), corroborating the hypothesis that cytotoxicity and genotoxicity may be related to oxidative stress.

Another study (Gibson et al., 2007; Hara et al., 1997; Krishnan and Bastow, 2000) demonstrated that eleutherin inhibits human TOPO II activity, stabilizing the complex DNA enzyme in the presence of ATP. In order to understand whether the greatest toxicity of eleutherin, in relation to isoeleutherin, is related to stabilizing the TOPO II-DNA complex, docking of the two molecules was carried out.

The difference between eleutherin and isoeleutherin observed in our study is due to the fact that they are optical isomers, and when they interact with molecular target, they do it differently due to the chiral carbon, generating an asymmetry, and thus differences in complementarity with the receptor, what happened with thalidomide, which in its isomeric form R (R-(+)Thalidomide) has a pharmacological effect, while its S (S-(-)-Thalidomide) isomer has the toxic effect, responsible for cases of teratogeny (Nemer and Khalil, 2019).

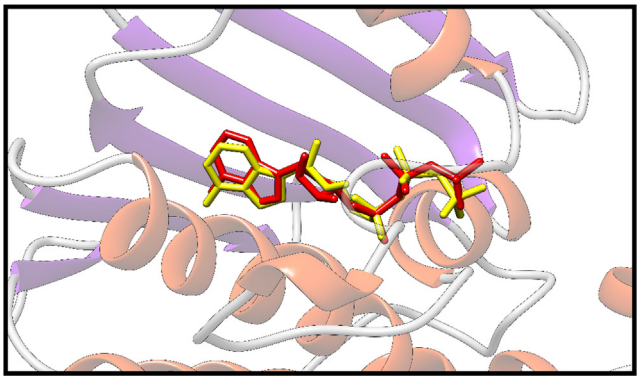

Fig. 4 The structure obtained by redocking (yellow), and overlapping the crystallographic structure (red) of TOPO II-bound complex.

3.3. Molecular docking and MD simulation results

To validate our docking methodology, we attempted to demonstrate that the conformation of the interaction between the co-crystallized ligand and TOPO II can be reproduced *in silico*. For this, the co-crystallized compound AMPPNP (phosphoaminophosphonic acid-adenylate ester) was redocked in the protein binding pocket using MVD 5.5. The fitness evaluation of each redocked pose was evaluated by considering the present root mean square deviation (RMSD) values and docking scores. According to literature, the binding mode prediction using docking should present a RMSD value <2.0 Å when superimposed on the crystallographic pose of the ligand (Araújo et al., 2020; dos Santos et al., 2020; Leão et al., 2020; Mascarenhas et al., 2020; Santos et al., 2020) (see Fig. 4).

The docking methodology has been successfully used to investigate the interaction of naturally occurring compounds with different molecular targets (Araújo et al., 2020; Costa et al., 2020; Lima et al., 2020; Pinto et al., 2019; Santana de Oliveira et al., 2020). After validating the docking methodology, the interaction mode and the connection affinity of eleutherin and isoeleutherin with TOPO II were investigated.

The interaction affinity between the ligand and the molecular target is essential for biologivl processes, since the interactions established at the protein binding site are capable of determining biological recognition at the molecular level. Thus, the search for ligands with high affinity is essential for the selection of new inhibitors. Therefore, our docking results suggest that naphthoquinones are able to interact with TOPO II in a favorable way; that is, they are capable of forming stable complexes. Isoeleutherin and eleutherin were able to favorably interact with the molecular target with results of affinity energy (MolDock Score) of −93.41 and −90.21, respectively.

The interactions between ligands and residues of the catalytic cavity are essential for understanding their binding and inhibition mechanisms; therefore, the nature of each interac-

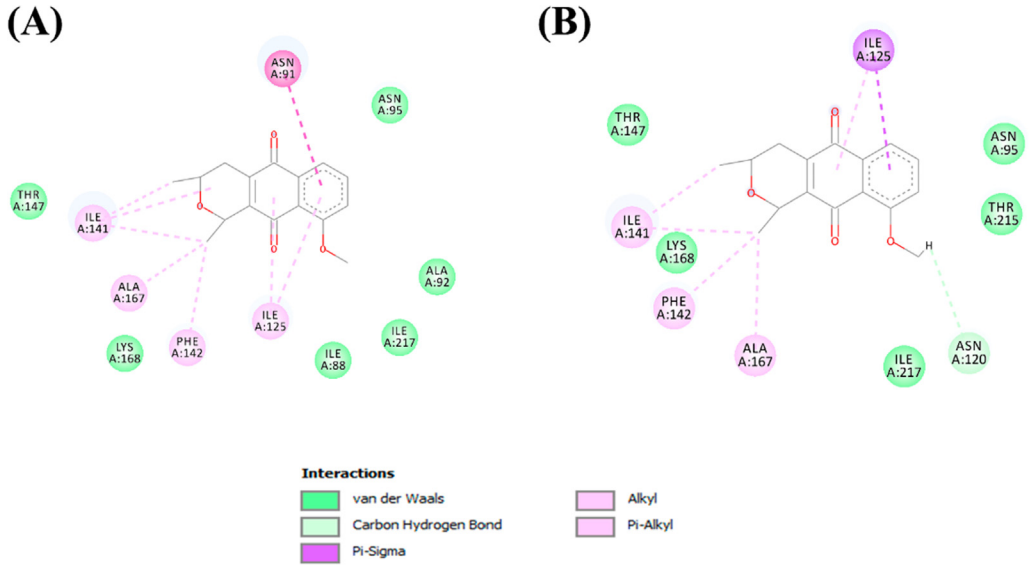

Fig. 5 Molecular interactions established between (A) Isoeleutherin and (B) eleutherin with the TOPO II binding pocket.

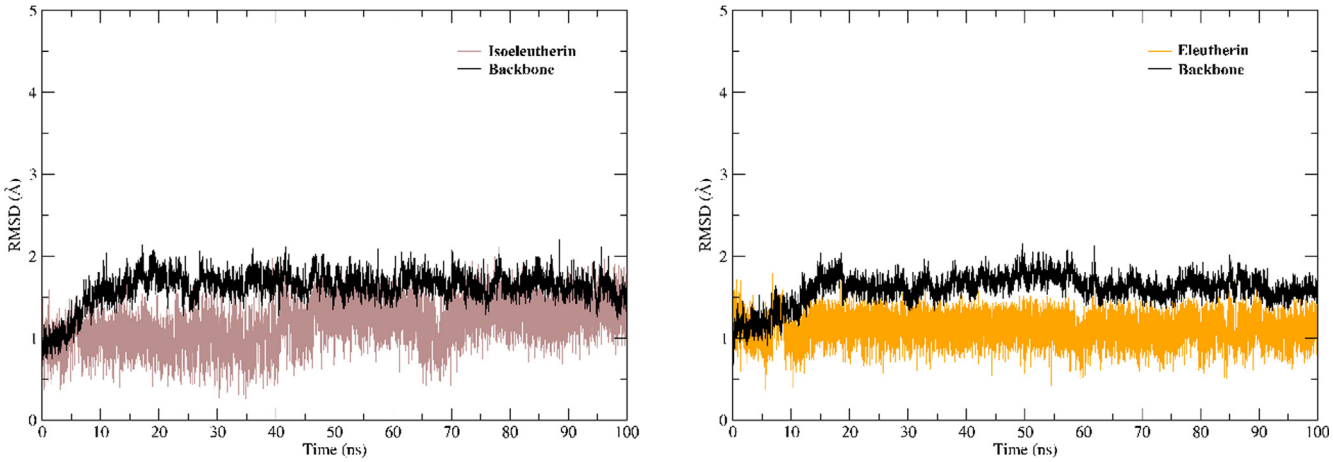

Fig. 6 RMSD plots. (A) RMSD plots for the complex established with isoeleutherin and (B) complex formed with eleutherin.

Table 4 Binding energy values and energy components. ΔEvdW, contributions by van der Waals interactions; ΔEele, electrostatic energy; ΔGGB, polar solvation energy; ΔGnp, nonpolar solvation energy; ΔGbind, binding affinity.

Inhibitor	ΔE_{vdW}[a]	ΔE_{ele}[a]	ΔG_{pol}[a]	ΔG_{nonpol}[a]	ΔG_{bind}[a]
Isoeleutherin	−44.13 ± 0.05	−12.66 ± 0.06	25.80 ± 0.04	−5.52	−36.52 ± 0.05
Eleutherin	−46.18 ± 0.06	−10.94 ± 0.05	20.48 ± 0.04	−5.16	−41.81 ± 0.07

[a] Values in kcal/mol.

tion of the compounds with TOPO II has been investigated and described.

In Fig. 5, we have the interactions established between isoeleutherin and eleutherin with the residues belonging to the binding pocket of TOPO II.

The main interactions established in the two complexes were hydrophobic in nature. Isoeleutherin established a pi-sigma interaction with the Asn91 residue. With Ile141, Ala167, and Phe142, alkyl type interactions were formed. Pi-alkyl interactions were formed with Ile125. Van der Waals interactions were established with the residues of Thr147, Lys168, Ile88, Ile217, Ala92, and Asn95. Eleutherin formed a hydrogen bond with Asn120, while with The147, Lys168, Ile217, Thr515, and Asn95, van der Waals interactions were formed. Ile125 formed a pi-sigma interaction with eleutherin, and the residues of Ile141, Phe142, and Ala167 established interactions of the alkyl type.

MD simulations were performed using the complexes obtained through molecular docking as a starting point. To evaluate the conformational changes of the complex, the trajectories of 100 ns were evaluated using the graphs of Root Mean Square deviation (RMSD). To plot the protein backbone graph, C alpha, C, O, and N atoms were used, while all heavy atoms were used to plot the ligand RMSD. In Fig. 6, we can see the RMSD graphs of the two complexes.

The RMSD graphs show that the ligands showed conformational stability along the MD trajectories. Both the ligands continued to interact with the protein until the end of the molecular dynamic simulations. In addition, the binders also showed values of free energy of favorable interaction with a value of −36.52 for isoeleutherin and −41.81 for eleutherin (Table 4).

4. Conclusions

The present study demonstrated that *in silico*, which isoeleuterine and eleuterine, have the same toxicity profile for marine organisms, hERG, mutagenicity and carcinogenicity. However, in the *Allium cepa* model, eleutherin caused a higher percentage of chromosomal aberrations than isoeleutherin, when compared to the positive control (12.5 μg/mL in 72 h), eleutherin caused a higher rate of chromosomal aberrations. In order to evaluate the low genotoxic potential of isoeleutherin, the micronucleus assay was performed, in which a low micronucleus frequency was verified, validating the results of the *Allium cepa*. The results of docking and MD simulations showed that the compounds interacted with the residues of the TOPO II binding pocket through hydrophobic interactions. Along the trajectories, the ligands remained in the active site of the protein and presented favorable values of affinity energy for the formation of the receptor-ligand complex. Thus, this study provides information for a better understanding of the genotoxicity and mutagenicity of isoeleutherin and eleutherin, in addition to demonstrating the interaction of these compounds with TOPO II.

Declaration of Competing Interest

The authors declare that they have no known competing financial interests or personal relationships that could have appeared to influence the work reported in this paper.

Acknowledgements

This study was financed in part by the Coordination of Superior Level Staff Improvement (CAPES) National Council for Scientific and Technological Development (CNPq) and PROPESP-UFPA.

Appendix A. Supplementary material

Supplementary data to this article can be found online at https://doi.org/10.1016/j.arabjc.2021.103084.

References

Araújo, P.H.F., Ramos, R.S., da Cruz, J.N., Silva, S.G., Ferreira, E.F. B., de Lima, L.R., Macêdo, W.J.C., Espejo-Román, J.M., Campos, J.M., Santos, C.B.R., 2020. Identification of potential COX-2 inhibitors for the treatment of inflammatory diseases using molecular modeling approaches. Molecules 25, 4183. https://doi.org/10.3390/molecules25184183.

Babula, P., Mikelova, R., Adam, V., Kizek, R., Havel, L., Sladky, Z., 2006. Using of liquid chromatography coupled with diode array detector for determination of naphthoquinones in plants and for investigation of influence of pH of cultivation medium on content of plumbagin in Dionaea muscipula. J.Chromatogr. B Anal. Technol. Biomed. Life Sci. 842, 28–35. https://doi.org/10.1016/j.jchromb.2006.05.009.

Bagatini, M.D., Ferreira Da Silva, A.C., Tedesco, S.B., 2007. The use of Allium cepa test as a bioindicator of genotoxicity of medicinal plants infusions. Brazil. J. Pharmacogn. https://doi.org/10.1590/s0102-695x2007000300019.

Bamford, M., Walkinshaw, G., Brown, R., 2000. Therapeutic applications of apoptosis research. Exp. Cell Res. 256, 1–11. https://doi.org/10.1006/excr.2000.4837.

Becke, A.D., 1993. Density-functional thermochemistry. III. The role of exact exchange. J. Chem. Phys. 98, 5648–5652. https://doi.org/10.1063/1.464913.

Bianchi, J., Mantovani, M.S., Marin-Morales, M.A., 2015. Analysis of the genotoxic potential of low concentrations of Malathion on the Allium cepa cells and rat hepatoma tissue culture. J. Environ. Sci. (China) 36, 102–111. https://doi.org/10.1016/j.jes.2015.03.034.

Campos, A., Barbosa Vendramini-Costa, D., Francisco Fiorito, G., Lúcia Tasca Gois Ruiz, A., Ernesto De Carvalho, J., Maria Rodrigues De Souza, G., Delle-Monache, F., Cechinel Filho, V., 2016. Antiproliferative effect of extracts and pyranonaphthoquinones obtained from Cipura paludosa bulbs. Pharm. Biol. 54, 1022–1026. Doi: 10.3109/13880209.2015.1091847.

Campos, V.R., Dos Santos, E.A., Ferreira, V.F., Montenegro, R.C., De Souza, M.C.B.V., Costa-Lotufo, L. V., De Moraes, M.O., Regufe, A.K.P., Jordão, A.K., Pinto, A.C., Resende, J.A.L.C., Cunha, A.C., 2012. Synthesis of carbohydrate-based naphthoquinones and their substituted phenylhydrazono derivatives as anticancer agents. RSC Adv. 2, 11438–11448. Doi: 10.1039/c2ra21514d.

Cornell, W.D., Cieplak, P., Bayly, C.I., Kollman, P.A., 1993. Application of RESP charges to calculate conformational energies, hydrogen bond energies, and free energies of solvation. J. Am. Chem. Soc. 115, 9620–9631. https://doi.org/10.1021/ja00074a030.

Costa, C.R., Olivi, P., Botta, C.M.R., Espindola, E.L.G., 2008. Toxicity in aquatic environments: discussion and evaluation methods. Quim. Nova 31, 1820–1830. https://doi.org/10.1590/S0100-40422008000700038.

Costa, E.B., Silva, R.C., Espejo-Román, J.M., Neto, M.F. de A., Cruz, J.N., Leite, F.H.A., Silva, C.H.T.P., Pinheiro, J.C., Macêdo, W.J.C., Santos, C.B.R., 2020. Chemometric methods in antimalarial drug design from 1,2,4,5-tetraoxanes analogues. SAR QSAR Environ. Res. 1–19. Doi: 10.1080/1062936X.2020.1803961.

Couto, C.L.L., Moraes, D.F.C.C., Do, M., Cartágenes, S.S., Do Amaral, F.M.M., Guerra, R.N., Cartágenes, M. do S.S., Amaral, F.M.M. do, Guerra, R.N., 2016. Eleutherine bulbous (Mill.) Urb.: A review study. J. Med. Plants Res. 10, 286–297. Doi: 10.5897/JMPR2016.6106.

Da Silva, M.N., Ferreira, V.F., De Souza, M.C.B.V., 2003. An overview of the chemistry and pharmacology of naphthoquinones with emphasis on β-Lapachone and derivatives. Quim. Nova. Doi: 10.1590/s0100-40422003000300019.

Darden, T., York, D., Pedersen, L., 1993. Particle mesh Ewald: An N·log(N) method for Ewald sums in large systems. J. Chem. Phys. 98, 10089–10092. https://doi.org/10.1063/1.464397.

Dennington, R., Keith, T., Millam, J., 2009. GaussView, Version 5. Semichem Inc., Shawnee Mission. KS.

Dolinsky, T.J., Nielsen, J.E., McCammon, J.A., Baker, N.A., 2004. PDB2PQR: An automated pipeline for the setup of Poisson-Boltzmann electrostatics calculations. Nucleic Acids Res. 32, W665–W667. https://doi.org/10.1093/nar/gkh381.

dos Santos, K.L.B., Cruz, J.N., Silva, L.B., Ramos, R.S., Neto, M.F. A., Lobato, C.C., Ota, S.S.B., Leite, F.H.A., Borges, R.S., da Silva, C.H.T.P., Campos, J.M., Santos, C.B.R., 2020. Identification of novel chemical entities for adenosine receptor type 2a using molecular modeling approaches. Molecules 25, 1245. https://doi.org/10.3390/molecules25051245.

Fenech, M., 2000. The in vitro micronucleus technique. Mutat. Res. – Fundam. Mol. Mech. Mutagen. 455, 81–95. https://doi.org/10.1016/S0027-5107(00)00065-8.

Fenech, M., Morley, A.A., 1985. Measurement of micronuclei in lymphocytes. Mutat. Res. Mutagen. Relat. Subj. 147, 29–36. https://doi.org/10.1016/0165-1161(85)90015-9.

Gibson, J.S., Andrey, O., Brimble, M.A., 2007. A short enantioselective synthesis of the topoisomerase II inhibitor (+)-eleutherin. Synthesis (Stuttg) 2007, 2611–2613. https://doi.org/10.1055/s-2007-983841.

Guilhermino, L., Diamantino, T., Carolina Silva, M., Soares, A.M.V. M., 2000. Acute toxicity test with Daphnia magna: An alternative to mammals in the prescreening of chemical toxicity?. Ecotoxicol. Environ. Saf. 46, 357–362. https://doi.org/10.1006/eesa.2000.1916.

Hara, H., Maruyama, N., Yamashita, S., Hayashi, Y., Lee, K.H., Bastow, K.F., Chairul, Marumoto, R., Imakura, Y., 1997. Elecanacin, a novel new naphthoquinone from the bulb of Eleutherine americana. Chem. Pharm. Bull. 45, 1714–1716. Doi: 10.1248/cpb.45.1714.

Janeczko, M., Kubiński, K., Martyna, A., Muzyczka, A., Boguszewska-Czubara, A., Czernik, S., Tokarska-Rodak, M., Chwedczuk, M., Demchuk, O.M., Golczyk, H., Masłyk, M., 2018. 1,4-Naphthoquinone derivatives potently suppress Candida Albicans growth, inhibit formation of hyphae and show no toxicity toward zebrafish embryos. J. Med. Microbiol. 67, 598–609. https://doi.org/10.1099/jmm.0.000700.

Jorgensen, W.L., Chandrasekhar, J., Madura, J.D., Impey, R.W., Klein, M.L., 1983. Comparison of simple potential functions for simulating liquid water. J. Chem. Phys. 79, 926–935. https://doi.org/10.1063/1.445869.

Kiran Aithal, B., Sunil Kumar, M.R., Nageshwar Rao, B., Udupa, N., Satish Rao, B.S., 2009. Juglone, a naphthoquinone from walnut, exerts cytotoxic and genotoxic effects against cultured melanoma tumor cells. Cell Biol. Int. 33, 1039–1049. https://doi.org/10.1016/j.cellbi.2009.06.018.

Kollman, P.A., Massova, I., Reyes, C., Kuhn, B., Huo, S., Chong, L., Lee, M., Lee, T., Duan, Y., Wang, W., Donini, O., Cieplak, P., Srinivasan, J., Case, D.A., Cheatham, T.E., 2000. Calculating structures and free energies of complex molecules: Combining molecular mechanics and continuum models. Acc. Chem. Res. 33, 889–897. https://doi.org/10.1021/ar000033j.

Krishnan, P., Bastow, K.F., 2000. Novel mechanisms of DNA topoisomerase II inhibition by pyranonaphthoquinone derivatives - Eleutherin, α lapachone, and β lapachone. Biochem. Pharmacol. 60, 1367–1379. https://doi.org/10.1016/S0006-2952(00)00437-8.

Kumar, M.R.S., Aithal, K., Rao, B.N., Udupa, N., Rao, B.S.S., 2009. Cytotoxic, genotoxic and oxidative stress induced by 1,4-naphthoquinone in B16F1 melanoma tumor cells. Toxicol. Vitr. 23, 242–250. https://doi.org/10.1016/j.tiv.2008.12.004.

Le, M.H., Do, T.T.H., Phan, V.K., Chau, V.M., Nguyen, T.H Van, Nguyen, X.N., Bui, H.T., Pham, Q.L., Bui, K.A., Kim, S.S.H., Hong, H.-J.J., Kim, S.S.H., Koh, Y.-S.S., Kim, Y.H., Ha, L.M., Huyen, D.T.T., Kiem, P Van, Minh, C Van, Van, N.T.H., Nhiem, N.X., Tai, B.H., Long, P.Q., Anh, B.K., Kim, S.S.H., Hong, H.-J. J., Kim, S.S.H., Koh, Y.-S.S., Kim, Y.H., 2013. Chemical constituents of the rhizome of eleutherine bulbosa and their inhibitory effect on the pro-inflammatory cytokines production in lipopolysaccharide -stimulated bone marrow-derived dendritic cells. Bull. Korean Chem. Soc. 34, 633–636. https://doi.org/10.5012/bkcs.2013.34.2.

Leão, R.P., Cruz, J.V., da Costa, G.V., Cruz, J.N., Ferreira, E.F.B., Silva, R.C., de Lima, L.R., Borges, R.S., Dos Santos, G.B., Santos, C.B.R., 2020. Identification of new rofecoxib-based cyclooxygenase-2 inhibitors: A bioinformatics approach. Pharmaceuticals 13, 1–26. https://doi.org/10.3390/ph13090209.

Lee, C., Yang, W., Parr, R.G., 1988. Development of the Colle-Salvetti correlation-energy formula into a functional of the electron density. Phys. Rev. B 37, 785–789. https://doi.org/10.1103/PhysRevB.37.785.

Lee, S., Lee, I.H., Kim, H. joong, Chang, G.S., Chung, J.E., No, K.T., 2002. The PreADME Approach: Web-based program for rapid prediction of physico-chemical, drug absorption and drug-like properties. Euro QSAR 2002 – Des. Drugs Crop Prot. Process. Probl. Solut. 418–420.

Li, H., Robertson, A.D., Jensen, J.H., 2005. Very fast empirical prediction and rationalization of protein pK a values. Proteins Struct. Funct. Genet. 61, 704–721. https://doi.org/10.1002/prot.20660.

Lima, A. de M., Siqueira, A.S., Möller, M.L.S., Souza, R.C. de, Cruz, J.N., Lima, A.R.J., Silva, R.C. da, Aguiar, D.C.F., Junior, J.L. da S.G.V., Gonçalves, E.C., 2020. In silico improvement of the cyanobacterial lectin microvirin and mannose interaction. J. Biomol. Struct. Dyn. Doi: 10.1080/07391102.2020.1821782.

Lin, C.H., Huang, C.C., Wang, T.W., Wang, Y.J., Lin, P.H., 2007. Disparity in the induction of glutathione depletion, ROS formation, poly(ADP-ribose) polymerase-1 activation, and apoptosis by quinonoid derivatives of naphthalene in human cultured cells. Chem. Biol. Interact. 165, 200–210. https://doi.org/10.1016/j.cbi.2006.12.005.

Lzaguirre, J.A., Catarello, D.P., Wozniak, J.M., Skeel, R.D., 2001. Langevin stabilization of molecular dynamics. J. Chem. Phys. 114, 2090–2098. https://doi.org/10.1063/1.1332996.

Maier, J.A., Martinez, C., Kasavajhala, K., Wickstrom, L., Hauser, K. E., Simmerling, C., 2015. ff14SB: Improving the Accuracy of Protein Side Chain and Backbone Parameters from ff99SB. J. Chem. Theory Comput. 11, 3696–3713. https://doi.org/10.1021/acs.jctc.5b00255.

Malheiros, L.C. da S., de Mello, J.C.P., Barbosa, W.L.R., 2015. Eleutherine Plicata – Quinones and Antioxidant Activity, in: Phytochemicals – Isolation, Characterisation and Role in Human Health. InTech. Doi: 10.5772/59865.

Mascarenhas, A.M.S., de Almeida, R.B.M., de Araujo Neto, M.F., Mendes, G.O., da Cruz, J.N., dos Santos, C.B.R., Botura, M.B., Leite, F.H.A., 2020. Pharmacophore-based virtual screening and molecular docking to identify promising dual inhibitors of human acetylcholinesterase and butyrylcholinesterase. J. Biomol. Struct. Dyn., 1–10 https://doi.org/10.1080/07391102.2020.1796791.

Nemer, G., Khalil, A., 2019. A cautious note on thalidomide usage in cancer treatment: Genetic profiling of the tbx2 sub-family gene expression is required. Drug Res. (Stuttg) 69, 512–518. https://doi.org/10.1055/a-0873-3529.

Neto, R. de A.M., Santos, C.B.R., Henriques, S.V.C., Machado, L. de O., Cruz, J.N., da Silva, C.H.T. de P., Federico, L.B., Oliveira, E. H.C. de, de Souza, M.P.C., da Silva, P.N.B., Taft, C.A., Ferreira, I. M., Gomes, M.R.F., 2020. Novel chalcones derivatives with potential antineoplastic activity investigated by docking and molecular dynamics simulations. J. Biomol. Struct. Dyn. 1–13. Doi: 10.1080/07391102.2020.1839562.

Neves Cruz, J., Santana de Oliveira, M., Gomes Silva, S., Pedro da Silva Souza Filho, A., Santiago Pereira, D., Lima e Lima, A.H., de Aguiar Andrade, E.H., 2020. Insight into the Interaction Mechanism of Nicotine, NNK, and NNN with Cytochrome P450 2A13 Based on Molecular Dynamics Simulation. J. Chem. Inf. Model. 60, 766–776. Doi: 10.1021/acs.jcim.9b00741.

Paramapojn, S., Ganzera, M., Gritsanapan, W., Stuppner, H., 2008. Analysis of naphthoquinone derivatives in the Asian medicinal plant Eleutherine americana by RP-HPLC and LC-MS. J. Pharm. Biomed. Anal. 47, 990–993. https://doi.org/10.1016/j.jpba.2008.04.005.

Pinto, V. de S., Araújo, J.S.C., Silva, R.C., da Costa, G. V., Cruz, J.N., Neto, M.F.D.A., Campos, J.M., Santos, C.B.R., Leite, F.H.A., Junior, M.C.S., 2019. In silico study to identify new antituberculosis molecules from natural sources by hierarchical virtual screening and molecular dynamics simulations. Pharmaceuticals 12, 36. Doi: 10.3390/ph12010036.

Prameela, R., Swamy, J., Venkaiah, M., 2018. Eleutherine bulbosa (Mill.) Urb. (Iridaceae): A new distributional record to the flora of Eastern Ghats. India. Trop. Plant Res. 5, 303–305. https://doi.org/10.22271/tpr.2018.v5.i3.038.

Ryckaert, J.P., Ciccotti, G., Berendsen, H.J.C., 1977. Numerical integration of the cartesian equations of motion of a system with constraints: molecular dynamics of n-alkanes. J. Comput. Phys. 23, 327–341. https://doi.org/10.1016/0021-9991(77)90098-5.

Salomon-Ferrer, R., Case, D.A., Walker, R.C., 2013. An overview of the Amber biomolecular simulation package. Wiley Interdiscip. Rev. Comput. Mol. Sci. 3, 198–210. https://doi.org/10.1002/wcms.1121.

Santana de Oliveira, M., da Cruz, J.N., Almeida da Costa, W., Silva, S.G., Britoda, M.P., de Menezes, S.A.F., de Jesus Chaves Neto, A. M., de Aguiar Andrade, E.H., de Carvalho Junior, R.N., OliveiraDe, M.S., Neves, J., Almeida, W., Silva, S.G., Brito, P., Augusto, S., MenezesDe, F., Nunes, R., Junior, D.C., 2020. Chemical composition, antimicrobial properties of Siparuna guianensis essential oil and a molecular docking and dynamics molecular study of its major chemical constituent. Molecules 25, 3852. https://doi.org/10.3390/molecules25173852.

Santos, C.B.R., Santos, K.L.B., Cruz, J.N., Leite, F.H.A., Borges, R. S., Taft, C.A., Campos, J.M., Silva, C.H.T.P., 2020. Molecular modeling approaches of selective adenosine receptor type 2A agonists as potential anti-inflammatory drugs. J. Biomol. Struct. Dyn. https://doi.org/10.1080/07391102.2020.1761878.

SivaKumar, V., Prakash, R., Murali, M.R., Devaraj, H., Devaraj, S. N., 2005. In vivo micronucleus assay and GST activity in assessing genotoxicity of plumbagin in Swiss albino mice. Drug Chem. Toxicol. 28, 499–507. https://doi.org/10.1080/01480540500263019.

Sunassee, S.N., Veale, C.G.L., Shunmoogam-Gounden, N., Osoniyi, O., Hendricks, D.T., Caira, M.R., De La Mare, J.A., Edkins, A.L., Pinto, A.V., Da Silva Júnior, E.N., Davies-Coleman, M.T., 2013. Cytotoxicity of lapachol, β-lapachone and related synthetic 1,4-naphthoquinones against oesophageal cancer cells. Eur. J. Med. Chem. 62, 98–110. https://doi.org/10.1016/j.ejmech.2012.12.048.

Thomsen, R., Christensen, M.H., 2006. MolDock: A new technique for high-accuracy molecular docking. J. Med. Chem. 49, 3315–3321. https://doi.org/10.1021/jm051197e.

Vale, V.V., Vilhena, T.C., Trindade, R.C.S., Ferreira, M.R.C., Percário, S., Soares, L.F., Pereira, W.L.A., Brandão, G.C., Oliveira, A.B., Dolabela, M.F., De Vasconcelos, F., 2015. Anti-

malarial activity and toxicity assessment of Himatanthus articulatus, a plant used to treat malaria in the Brazilian Amazon. Malar. J. 14, 132. https://doi.org/10.1186/s12936-015-0643-1.

Vale, V.V., Cruz, J.N., Viana, G.M.R., Póvoa, M.M., Brasil, D. do S. B., Dolabela, M.F., 2020. Naphthoquinones isolated from Eleutherine plicata herb: in vitro antimalarial activity and molecular modeling to investigate their binding modes. Med. Chem. Res. 29, 487–494. Doi: 10.1007/s00044-019-02498-z.

Wang, J., Wang, W., Kollman, P.A., Case, D.A., 2006. Automatic atom type and bond type perception in molecular mechanical calculations. J. Mol. Graph. Model. 25, 247–260. https://doi.org/10.1016/j.jmgm.2005.12.005.

Wang, J., Wolf, R.M., Caldwell, J.W., Kollman, P.A., Case, D.A., 2004. Development and testing of a general Amber force field. J. Comput. Chem. 25, 1157–1174. https://doi.org/10.1002/jcc.20035.

Wang, J.C., 1996. DNA topoisomerases. Annu. Rev. Biochem. 65, 635–692. https://doi.org/10.1146/annurev.bi.65.070196.003223.

Wei, H., Ruthenburg, A.J., Bechis, S.K., Verdine, G.L., 2005. Nucleotide-dependent domain movement in the ATPase domain of a human type IIA DNA topoisomerase. J. Biol. Chem. 280, 37041–37047. https://doi.org/10.1074/jbc.M506520200.

Zucker, E., 1985. Hazard Evaluation Division, Standar Evaluation Procedure - Acute toxicity test for freshwater fish. U.S. Environmental Protection Agency Office of Pesticide Programs, Washington D.C.